Article citation info:
Idzior M, Karpiuk W, Smolec R. Investigation of a novel ceramic materials (Al_2O_3 and SSiC) for high-pressure pumps' delivery sections. Combustion Engines. 2024;196(1):153-160. https://doi.org/10.19206/CE-174315

Marek IDZIOR
Wojciech KARPIUK
Rafal SMOLEC

Combustion Engines
Polish Scientific Society of Combustion Engines

Investigation of novel ceramic materials (Al_2O_3 and SSiC) for high-pressure pumps delivery sections

ARTICLE INFO

Received: 27 July 2023
Revised: 4 September 2023
Accepted: 19 October 2023
Available online: 23 November 2023

In this paper, a comparative analysis of structural materials used in the construction of high-pressure pumps delivery sections was carried out. The focus was on a comparison of the ceramic materials such as corundum (alumina, Al_2O_3) and silicon carbide (solid-state sintered) – SSiC with bearing alloy steel 100Cr6, that is the most common material used to make pistons and cylinders of the delivery section of common rail injection pumps. Simulations performed using the finite element method have proven that ceramic materials have a number of advantages and could therefore be an interesting substitute for materials traditionally used in this area.

Key words: *ceramic, injection systems, common rail, fuel pump, FEM*

1. Introduction

A common feature of the high-pressure pumps used in passenger cars from all manufacturers is the use of fuel as a lubricant. During pump operation, fuel is supplied to both the delivery sections and the drive train (shaft–cam). It is therefore necessary to ensure proper lubrication parameters that will allow the formation of an oil film and thus the separation of the cooperating surfaces.

The lubricity of fuels is determined using the HFFR method. It consists of determining the maximum diagonal imprint resulting from a ball wear test using the test fuel as a lubricant. Figure 1 shows the relationship between running time and wear on pump components (expressed in micrometres of material layer loss). Analyzing the data, a clear relationship can be seen between the HFFR parameter and the durability of pump components. If the HFFR is above 600 µm, there is a very rapid increase in wear, leading to the destruction of the pump. For this reason, the fuel delivered to filling stations must meet the requirements of the standard [21], which sets an upper limit for the HFFR parameter of 460 µm. It should be emphasized that the addition of rapeseed oil fatty acid methyl esters to diesel effectively improves its lubricating properties due to the very favorable HFRR coefficient, which for pure rapeseed oil fatty acid methyl esters is below 200 µm.

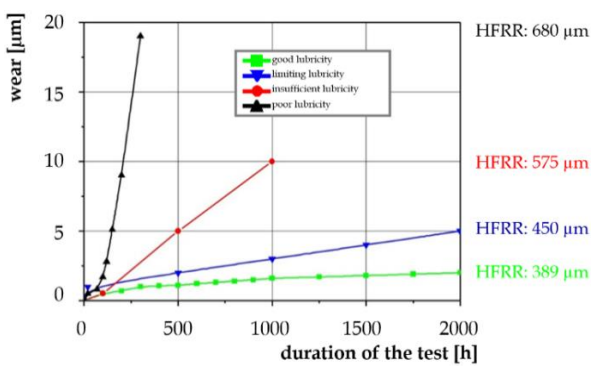

Fig. 1. The dependence of the wear of the pump components on the duration of the test [22]

One of the primary causes of pump failures is insufficient fuel quality. This conclusion is related to the lubricity issue described. It should be noted, however, that the inadequate design of both the low-pressure feed pump and the high-pressure pump is also a factor in the formation and progression of injection system failures. Thus, in terms of use, the increased forces occurring in the pump drive system must not translate into increased wear in the precision pair of cylinder and piston and the cam and tappet area. It is these structural components that are responsible for the pump's correct operation. Their durability can be increased by using modern materials in the field of engineering ceramics. To properly select such materials, it seems necessary to know the nature of their operation and the damage that occurs in their working area.

2. Causes of damage and functional problem

The main cause of wear in high-pressure injection systems is contamination. The destruction of precision components, whose steel surfaces are finely machined, is influenced by hard mineral particles (silica, alumina) [5]. They can get into the pump system in the form of impurities along with fuel or lubricating oil. Surface pressures in the case of tappet and roller or plain bearings are the result of the negative effect of excessive clearances and unevenness. This leads to a rapid expansion of wear, and the products, i.e. metal particles including steel, increase the amount of contamination in the lubricating oil and fuel. On the other hand, the formation of fretting corrosion is favored by water getting into the oil. Such a process significantly accelerates the wear of rubbing or rolling steel surfaces. As a result, hematite (Fe_2O_3), a product of wear, enters the fuel or lubricating oil, impairing its lubricating properties. It is often observed that the oil changes its consistency into a dense mixture of heavy hydrocarbons with impurities and water particles. This has a detrimental effect on mating pump components, causing deposits to form, e.g. on cylinder walls [5].

Damage to the surfaces of cams and eccentrics and the tappet rollers that roll over them is also a major problem. Particularly unfavorable are larger cavities, chipping of the

surface layer of metal, the presence of developed corrosion and localised collapsing of the cam distorting its profile, especially at the transition from the cam's tangential surface to its apex. The tappet spring is subject to surface scratching, corrosion and cracking. Other parts of the pump, the design of which depends on the variety and type of pump, are closely related to the potential for a variety of damage. They also depend on the operating conditions of the high-pressure pump. Such elements are: precision pairs, high pressure connections, hoses, valves, and control sleeves [5].

An example of a pump where the failure rate is mainly based on precision pair wear is the Bosch CP1 pump. This is only an example illustrating the problem – Siemens VDO pumps, for instance, are characterised by a similar design. In the case of the Bosch, the defect is caused by the negative effect of the design itself in combination with the load. The problem lies in the pivoting position of the tappet relative to the rotating cam on the pump shaft. This position of the tappet results in a tangential force to the cam in addition to the normal force. Under unfavorable conditions and insufficient lubrication, in addition to the force perpendicular to the piston axis, the frictional force has a negative effect [17]. This forces stresses into the mating components and results in material breakage. The resulting wear products can enter the piston-cylinder precision pairs, causing their destruction through abrasive wear and the formation of cracks (Fig. 2). Noticeable scratches then occur on the cylindrical surface of the piston, resulting, in a later stage of wear, in leakage in the working area of the pump [9, 18].

Fig. 2. Pump section piston with scratches on the side surface [10]

Torn-off material particles can also enter the part of the pump where the roller rotates. Material loss occurs on the side surface of the tappet due to the occurrence of cavitation and shearing due to contact between roughness vertices [11]. The cavitation mentioned can occur within the pump and high-pressure lines. It involves the formation of vapor bubbles due to the action of varying pressure and implosion, which, when occurring close to the walls, causes damage to the walls. The high energy density contributes to the formation of cavitation pits [11].

Some swarf also enters the high-pressure pump from the pre-pumping pump. This is usually a gear pump characterised by a discharge pressure of 300–600 kPa. The contact area between the teeth and the pump raceway is exposed to frictional forces resulting in tribological wear.

A sensitive area is the inlet and outlet valves from the delivery section. A frequent cause of damage in this area is particles from dirt in the pumped oil. The discharge valve is made up of a ball embedded in a seat. The loss of tightness of this association is caused by erosion and distortion of both components. Defects can also occur in the throttling hole safety valve used to distribute fuel between the discharge section and the pump's lubrication and cooling circuit, under the influence of pressure variations in the low-pressure circuit. Defects in this area result in reduced cooling of the delivery section and consequent heating of the components [11].

The drive shaft of the pump is also susceptible to damage. During the transmission via the coupling, run-out of the cam shaft can occur, as well as its rubbing under the sealing ring. Wear occurs at the point of connection between the shaft and the coupling (Fig. 3) [11]. The seals also deteriorate under pressure and contaminants present, resulting in fuel leaking outside the pump body. The high pressures generated by the pump contribute to high loads on the shaft itself and the eccentric placed on it, as well as on the plain bearings in the body. The highest loads from the pressure forces occur when reaching the top extreme position of the piston. The loads are transferred at the bearing locations. These are characterised by varying wear of the roller surfaces. Micro-cutting and furrowing occur at those locations adjacent to the shortest radius of the eccentric [1].

Fig. 3. Examples of damage to the pump cam shaft [10]

3. Ceramics as a material for precision pump pairs

For the material analysis, ceramic materials such as corundum (alumina, Al_2O_3) and silicon carbide (solid-state sintered) – SSiC were used and compared with 100Cr6 alloy bearing steel, i.e. the most popular of the materials from which the pistons and cylinders of the pumping sections of the pumps are made common rail injection system.

Alumina, also called corundum, especially in the stable polymorphic form alpha (α-Al_2O_3), is characterized by properties suitable for construction purposes [12, 18]. The variety mentioned here, crystallized in the hexagonal system, has good strength and tribological properties, although it should be mentioned that they depend on the course of the sintering process [8]. Valuable properties in terms of strength are also shown by silicon carbide, which is characterized by similar and even more favorable material parameters than Al_2O_3. Its advantages are greater hardness and

resistance to thermal shock, and better mechanical properties, including, for example, durability. When choosing a material for a specific application, its mechanical properties should be taken into account. The materials of the elements of precision pairs should behave appropriately under the influence of occurring loads.

Ceramic materials are prone to brittle fracture, which is different from metals, where a certain range of plastic deformation is noticeable. The reason lies in the structure of the ceramic, where the covalent bonds are directional. In addition, there are defects in the form of cracks, pores and voids, and the samples are destroyed already in the range of elastic deformations [8, 16]. These discontinuities in the structure contribute to a lower resistance to tensile loading and cracking due to tensile stresses that are lower than those assumed based on interatomic bonds. Then, the aforementioned empty spaces are expanded, which in turn leads to a reduction in the load-carrying capacity [15]. Ceramics are characterized by higher compressive strength compared to tensile strength ($R_c \cong 15 \cdot R_m$) [20]. Therefore, it is advantageous to use engineering ceramics in section pump pistons, but also in rollers, because due to the nature of work, these elements transfer compressive loads. The most important mechanical properties of the analyzed materials from the point of view of the conducted considerations are presented in Table 1.

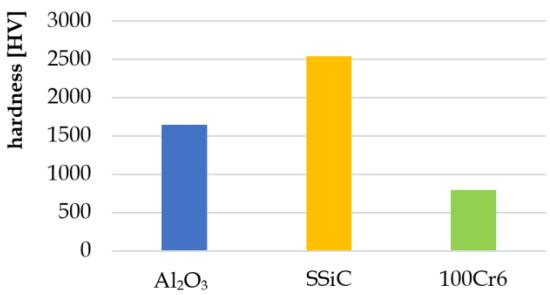

Fig. 4. Comparison of the hardness of ceramics and steels [24]

The characteristic features of ceramic materials are their high hardness and abrasion resistance. This is due to the structure in which the network with ionic bonds resists dislocations [19]. It is very difficult to initiate their movement, and permanent plastic deformation occurs through these linear defects. The determination of hardness by various available methods is also the determination of the state of plasticity, so it can be considered through deformation. To activate the dislocation, high stresses are needed in the tangential direction of the bonds, which results in their tearing [9]. The critical stress of alumina ceramics that initiates dislocation slipping is high, of the order of E/30, while for metals it is only E/1000 [3]. A comparison of the hardness of ceramics and steel is shown in Fig. 4. An analogous combination concerning Young's modulus is shown in Fig. 5.

In the case of Al_2O_3 alumina with ionic bonds, the movement of atoms in certain directions is complete, so the resistance is lower [3, 9]. Note the high hardness of SSiC, even greater than Al_2O_3, far exceeding the level typical for metals. The associated Young's modulus E, which determines the resistance to elastic deformation, is about 430 GPa. At the same time, it is not dependent on the load operation time. Hardness and strength, which are dependent properties, are affected by the type of structure-building bonds. As mentioned, these are covalent bonds resistant to activation and dislocation [23]. Like alumina, silicon carbide has a certain strength distribution, describing the possibility of failure even under stresses at which it should withstand the load.

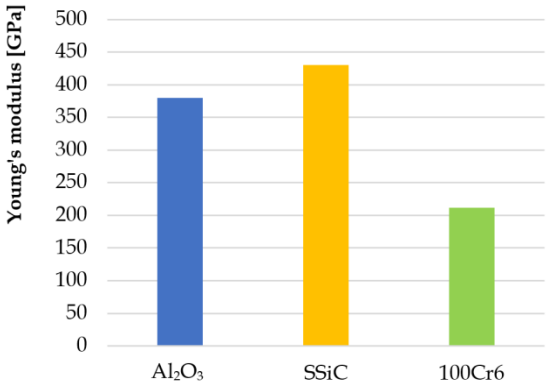

Fig. 5. Comparison of Young's modulus of ceramic materials and steel [24]

An important parameter from the point of view of injection pumps is the stress intensity factor K1C. Its value for ceramic materials is more than three times lower than for 100Cr6 steel. According to the definition of the parameter, this indicator determines the load causing uncontrolled crack development in sections [7]. This is the adverse effect of hindering dislocation slippage. Ceramic materials are characterized by lower fracture toughness than metals due to the limited plastic deformation capacity, and thus lower impact strength. The high brittleness of engineering ceramics can be the main obstacle in the structural applications of the designed elements. Products made of it are often destroyed during use or their premature damage is noticeable. It is therefore important to avoid structure discontinuities, e.g. micro-cracks, by maintaining a low tolerance for defects [14]. Even micro-scale cracks, within the tolerance range, smaller than critical cracks, can develop and contribute to their further propagation [20]. Compressive and flexural strengths should also be closely monitored – ceramic materials withstand pressure loads much better than metals [9, 14, 20, 25].

Table 1. Mechanical properties of the analyzed materials

Material	Standardised hardness HK0.1 [GPa]	Vickers hardness [HV]	Stress intensity factor K_{1C} [MPa $m^{1/2}$]	Compressive strength R_c [MPa]	Bending strength R_g [MPa]	Young's modulus E [GPa]
Al_2O_3	23	1650	4.2–6.0	3500	350	380
SSiC	24,5	2540	4.0	> 2500	400	430
100Cr6	–	800	15.4–18.7	–	–	212

The nature of the operation of precision pairs, i.e. sliding contact, imposes high demands on their surface resistance to various types of wear. The condition of the surface structure of products plays a key role in the issue of abrasion. Roughness is also important, but in the case of engineering ceramics, there are some limitations in this respect. The reason is the occurrence of "losses" of the material, i.e. voids, pores, etc., which significantly change the distribution of the surface layer. However, the description of the surface is made possible by other parameters related to load capacity, lubricant capacity (R_{pk}, R_k, R_{vk}), etc. The study of ceramic wear shows the conclusion [4] that the final surface treatment is an important aspect, significantly influencing the roughness. The structure of aluminum oxide depends on the sintering process, the average grain diameter is about 7.5 µm. On the other hand, for SSiC, this value is at the level of about 1.9 µm, so Al_2O_3 is characterized by greater roughness. At the same time, however, both materials show relatively deep defects due to grain tearing, although the number of defect cavities is smaller on the surface of the alumina subjected to polishing.

The parameter determining the quality of the surface is, among others, the coefficient of friction, which plays an important role in the fitting of elements of precision pairs. In common rail injection pumps, a long surface cover is used, which significantly affects the tightness of the node and reduces losses. Unfortunately, the accuracy of the fit increases the contact area of the surfaces and the resistance to movement, and also causes the occurrence of increased phenomena such as heat release. The presence of liquid in the mating pair is also important aspect. The use of ceramic materials should also be considered in above mentioned areas. It is important to reduce the coefficient of friction, which increases the efficiency of the system, but also minimizes the possibility of wear.

The hardness of the surface has a significant impact on the elements in the friction node. Increasing the value of this parameter minimizes the negative effects of tribological processes, including abrasion. The use of ceramic materials leads to the elimination of tribochemical wear, so no adhesive bonds are leading to seizing of the piston-cylinder friction node.

Another issue worth mentioning concerning the use of engineering ceramics in high-pressure injection systems is their chemical and corrosion resistance. Ceramic materials achieve significant resistance even at high operating temperatures, which becomes important in various demanding applications. What is important then is the oxidation process. However, in this system, there is only elevated temperature, because the diesel fuel in the injection pump reaches temperatures of 60°C.

4. Simulation of precision pair operation with results

In the initial preparation for the simulation, the piston-cylinder system of the Bosch CP3 and CP4 pumps was analysed. The difference between the two is the way the motion is transmitted to the piston. In the CP3 pump (Fig. 6), the reciprocating movement is forced by an eccentric on the glass tappet mechanism. In CP4, the movement is forced by a roller (Fig. 7).

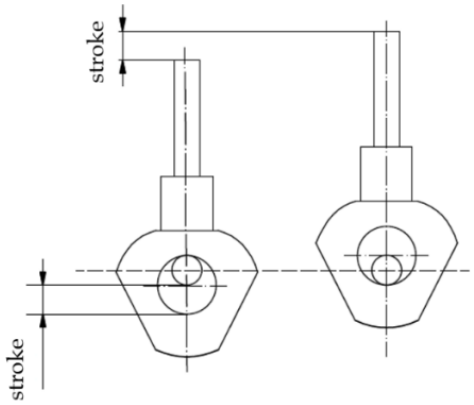

Fig. 6. Principle of operation of the pumping section of the CP3 pump

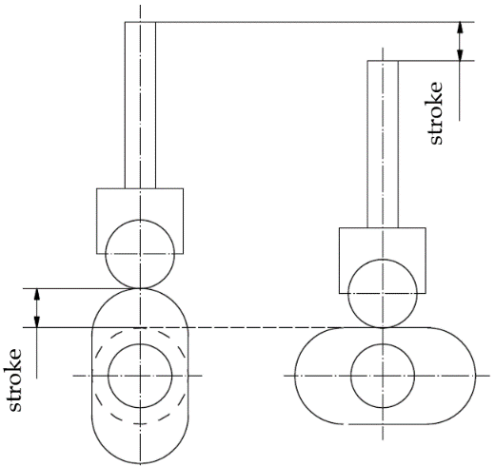

Fig. 7. Principle of operation of the pumping section of the CP4 pump

The course of the piston lift during the entire operating period is variable with some momentary constant values during the supply of fuel to the cylinder's working volume (Fig. 8).

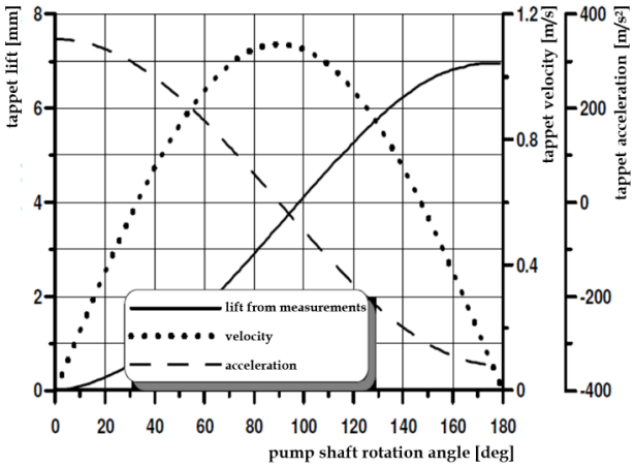

Fig. 8. Diagram of the dependence of lift, velocity and acceleration of the tappet on the angle of rotation of the CP3 pump shaft [6]

It moves from the inlet valve to the bottom dead center, below the high-pressure outlet valve. Thus, the volume of the pumped fuel depends geometrically on the position of the piston during its operation – for the assumed typical dimensions of the section, it varies from 100 to 250 mm^3.

During full load, after a certain period, the initial volume is already approx. 123 mm^3 [6]. The movement of the piston enables the generation of pressures in the CP3 pump up to approx. 180 MPa. The maximum value is reached at the initial pressure resulting from the operation of the feeding pump is about 0.7 MPa. The newer generation of the pump already can generate a pressure of about 200 MPa. The design of the piston must withstand such high pressure loads. Both pumps are devoid of construction defects that occurred in the CP1 generation discussed in Chapter 2. A roller or bucket tappet mechanism avoided the occurrence of forces transverse to the piston axis caused by a sliding plate tappet. This resulted in wear on the lateral surfaces, including the cylinder. Ceramic materials, which are not resistant to bending and are prone to fracture, may not have fulfilled their role in this application [13].

The geometry of the CP4 pump head was used for further finite element analysis. A schematic of the pump model including the components (head, piston, cylinder) is shown in Fig. 9.

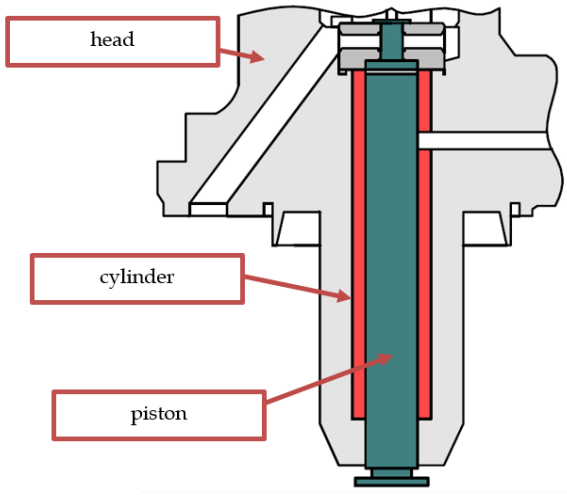

Fig. 9. Model of a CP4 pump

This assumed the use of ceramic materials in the piston-cylinder junction as respectively made junction pairs: Al_2O_3/Al_2O_3 or, in the second variant, SSiC/SSiC. It was further assumed that both components were made by powder metallurgy methods – sintering, while the mating surfaces themselves were subjected to grinding, achieving low surface roughness. The piston and cylinder model used for the simulation, is shown in Fig. 10.

The CAD model of the pump piston used in the simulations was made in the Autodesk Inventor environment. The simulation in this area, using FEM, was realised in the Nastran In Cad package. The discretisation of the piston allowed the model to be divided into finite elements and nodes, by determining a finite element size reduction run for the entire geometry. The model was divided into 35,584 finite elements and 55,426 nodes (Fig. 11).

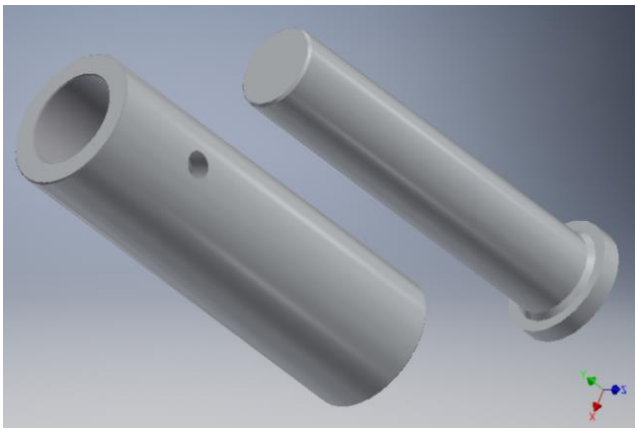

Fig. 10. Piston and cylinder model used for the simulation

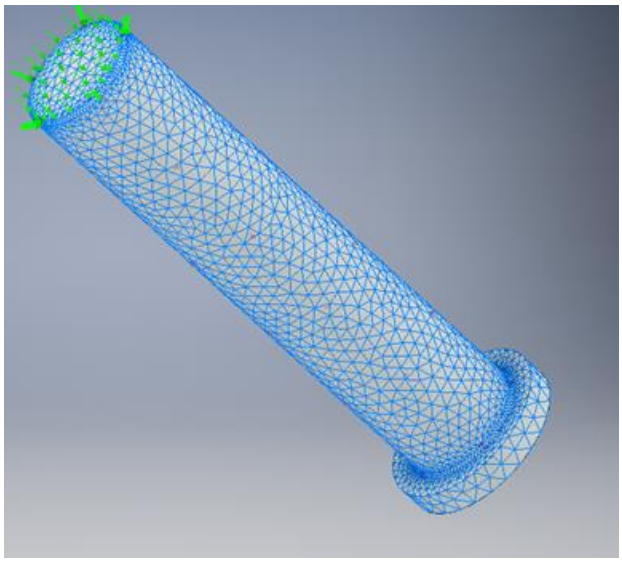

Fig. 11. Piston model discretised into finite elements

It was assumed that the analysis would replicate the conditions prevailing at maximum load, however, the effects of the cylinder/pump head were ignored. For this reason, the piston is subjected to a higher load than the actual load. The interaction of the spring thrust plate with the piston shoe has also been omitted – so the main focus is on the pressure action and its effects. Accordingly, the piston was subjected to the highest possible pressure that was assumed to exist in the pump, i.e. 180 MPa at the end of the compression stroke. The pressure force was applied to the top surface of the piston and the bottom surface of the bead was restrained. The simulation was carried out for three variations of the component design. The first material was corundum the second material was silicon carbide (solid-state sintered) – SSiC, the third material was 100Cr6 alloy-bearing steel.

The material properties were determined based on reference materials [2, 7]. It was decided to collect the results at the moment of the highest discharge pressure, with the assumed course of its variation, as this is a variable load analysis for the moment 0.02 s when the maximum was reached.

An example of simulation results for a component made of sintered silicon carbide is presented in Fig. 12 and 13.

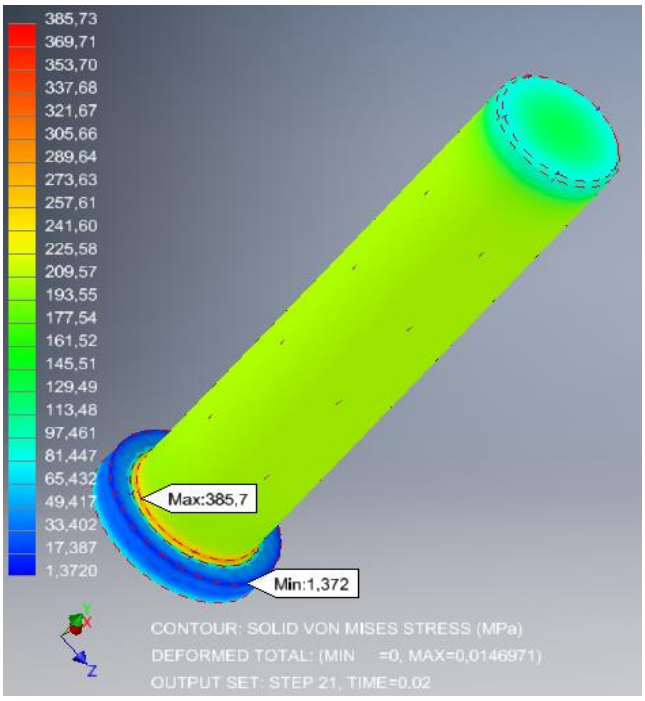

Fig. 12. Huber-Misses reduced stress distribution [MPa] for a component made of made of SSiC

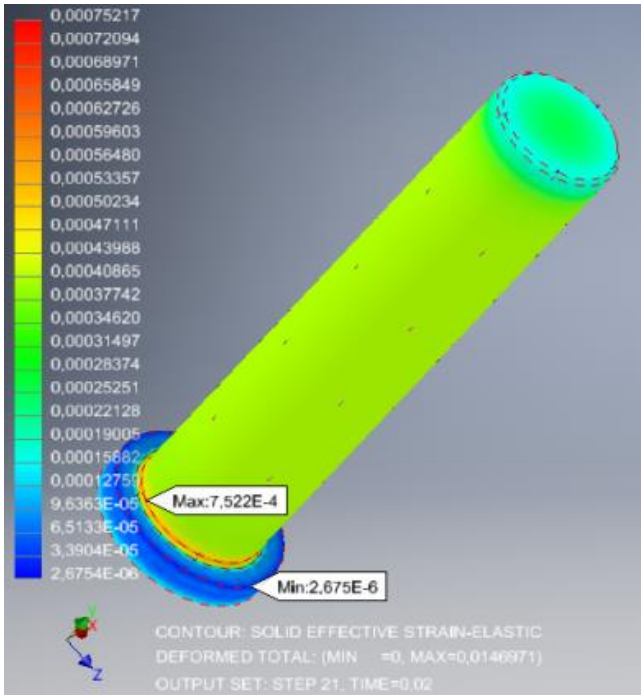

Fig. 13. Strain distribution [-] for a component made of SSiC

Through the finite element computational environment, the feasibility of using Al_2O_3 and SSiC ceramic materials and 100Cr6 steel was analysed. The time-varying load analysis was generalised as a static compression test, thus a strictly strength simulation, and this was adopted in further inference. The set of results is illustrated in Table 2.

The concentration of the maximum stress results for all variants of the component design falls within the area of geometric change. For bearing steel, the smallest maximum reduced stress was obtained, as metals, unlike ceramics, are characterised by elastic and plastic periods. In contrast, as in the other cases, the clustering of the highest stresses and strains occurs just at the transition of the piston geometry to its bead. In this case, the reduced stresses exceed the value of the allowable stresses calculated analytically according to relation (1).

$$\sigma_{dop} = (0.55 - 0.65)R_e \tag{1}$$

Table 2. Results of the analyses

	Al_2O_3	SSiC	100Cr6
Huber-Misses maximum reduced stresses [MPa]	373.4	385.7	372.8
Maximum strain [–]	0.000852	0.000752	0.001539

For compression, the parameter R_e has approximate values determined from the tensile test. In the analysis, a yield strength of 400 MPa was determined for 100Cr6 steel, for which, according to the above relationship, the allowable stress is in the range 220–260 MPa. The maximum simulation result was 372.8 MPa, and condition (2) was not met.

$$\sigma_{red} < \sigma_{dop} \tag{2}$$

The occurrence of maximum stresses in this area of the component can cause the structure to weaken, and the maximum deformation with respect to the entire component indicates that this area is subject to some plastic deformation. This is confirmed by numerous examples of piston damage. Most often, material swelling occurs in this area as a result of plastic deformation caused by the generation of pressures up to their maximum value and the cyclic nature of these pressures – the internal stresses then exceed the permissible values. The resulting load cycles cause fatigue, which can result in cracks forming in the plasticisation zone. It is clear that plastic deformation can result from friction between piston and cylinder, inhomogeneities in material strengthening, uneven temperature distribution and the influence of strain rate. The effects of such a process are changes in the properties of the structure, and (under appropriate geometric conditions) swelling. This may result in slight changes in the diameter of the piston, which directly affects its function – the friction of the mating surfaces. It should be noted, however, that the yield strength considered to illustrate an example of this type of bearing steel can be higher, for example, when hardening is applied. R_e then reaches a value of approximately 1300 MPa.

5. Summary

The paper compares selected ceramic materials Al_2O_3 and SSiC with 100Cr6 steel. Particular attention was paid to the use of the above materials in the precision pairs of a common rail injection pump. A simulation was carried out using FEM by inducing a load on the upper part of the piston, which was assigned the properties of the three compared materials.

The results of the example simulation show that the level of deformation in ceramic components is lower than in metal. In ceramics, plastic deformation does not occur under load, and failure occurs through brittle fracture. The

strain level of Al_2O_3 and SSiC ceramics in this analysis was smaller by an order of magnitude.

Taking the compressive strength as equivalent to the tensile strength (such a simplification is reasonable when describing elastic-plastic materials), a significant advantage of ceramics over steel is noted. The compressive strength of Al_2O_3 and SSiC is higher than that of 100Cr6 steel, even when subjected to processes that increase the overall strength parameters. It is also possible to determine analytically the allowable stresses if the yield strength (Re) is replaced by the compressive strength in formula (1). In this way, the clear limit of the value after which failure (fracture) of the material will occur is much higher than those presented by metals. On the other hand, the fracture itself may occur below the allowable stress values – with regard to ceramics, this is a particularly noteworthy strength aspect.

The results of the analysis mainly depend on the adopted elasticity constants of the material: Young's modulus (E) and Poisson's number. For a constant surface perpendicular to the applied pressure, and therefore for a constant piston diameter, the deformation in the test depends on the longitudinal modulus of elasticity. The greater its value, the smaller the deformation will be and the more rigid the component. For ceramics, this modulus is significantly higher than for steel, as can be seen in the analysis results.

The inhomogeneous structure of ceramics, or more precisely, the pores present in them, is the reason for the appearance of notches, where stresses are concentrated to varying degrees. The simulation does not take into account the presence of defects in the structure, i.e. cracks, pores, voids. It should be emphasized that the analysis carried out is a certain simplification, as parts with a more complex structure and irregular pores may have different stress and strain field distributions that are more difficult to determine properly. This simplification was made because stress concentrations caused by the presence of structural defects are not taken into account for compressive stresses. This means that a component such as a piston subjected mainly to a compressive force is not affected by internal defects, because with such an actual condition the pores are closing and not opening [18].

Nomenclature

SSiC	sintered silicon carbide	FEM	finite element method
HFRR	high frequency reciprocating rig		

Bibliography

[1] Bajerlein M, Bor M, Karpiuk W, Smolec R, Spadlo M. Strength analysis of critical components of high-pressure fuel pump with hypocycloid drive. B Pol Acad Sci Tech. 2020;68(6):1341-1350. https://doi.org/10.24425/bpasts.2020.135380

[2] Blicharski M. Material engineering (PL original: Inżynieria materiałowa). WNT. Warsaw 2019.

[3] Clifton B. Ultracoatings: Enabling energy and power solutions in high contact stress environments through next-generation nanocoatings. CRADA Final Report 2012.

[4] Dulias U, Zum Gahr K-H. Investigation of Al_2O_3 and SSiC-ceramic under lubricated, reciprocating sliding contact and cavitation erosion. Materialwiss Werkst. 2005;36(3-4):140-147. https://doi.org/10.1002/mawe.200500860

[5] Falkowski H, Krępeć T. Maintenance and repair of diesel engine fuel apparatus. WKiL. Warsaw 1973.

[6] Gancarczyk T, Knefel T. Model analysis of the high pressure pump of a common rail system. Mechanik. 2013;86.

[7] Golewski GL. Stress intensity factor as a basic parameter for assessing the fracture toughness of concrete composites. Drogownictwo. 2010;1:31-35.

[8] Ji R, Yao Z, Zhang Y, Wang R. Effects of nano-ceramic coatings on the thermal structure of ω-type pistons. Chinese Intern Combust Engine Eng. 2023;44(2):51-57. https://doi.org/10.13949/j.cnki.nrjgc.2023.02.007

[9] Kaczorowski M, Krzyńska A. Structural metallic, ceramic and composite materials. 2nd ed. Warsaw Technical University Publishing House. Warsaw 2017.

[10] Karpiuk W. Study of the design of a hypocycloidal injection pump. Poznan University of Technology Publishing House. Poznan 2022.

[11] Kruczyński S, Chrupek B. Malfunctions of the common rail fuel system of modern compression-ignition engines Zeszyty Naukowe Instytutu Pojazdów. Warsaw 2014.

[12] Li R, Chen Q, Ouyang L, Ding Y. Adhesion strength and bonding mechanism of γ-Fe (111)/α-Al_2O_3 (0001) interfaces with different terminations. J Alloy Compd. 2021;870:159529. https://doi.org/10.1016/j.jallcom.2021.159529

[13] Magryta P, Pietrykowski K. Crankshaft geometry modification and strength simulations for a new design of diesel opposed-piston engine. Combustion Engines. 2023;194(3):123-128. https://doi.org/10.19206/CE-169371

[14] Majeed EA, Rashid HK, Hussain MK. Review of ceramic materials that used as a thermal barrier in diesel engine pistons. J Phys Conf Ser. 2021;1973:012125. https://doi.org/10.1088/1742-6596/1973/1/012125

[15] Matizamhuka WR. Advanced ceramics – the new frontier in modern-day technology: Part I. J S Afr I Min Metall. 2018;118:757-764. https://doi.org/10.17159/2411-9717/2018/v118n7a9

[16] Mercier JP, Zambelli G, Kurz W. Introduction to Materials Science. Elsevier 2003. https://doi.org/10.1016/C2009-0-29148-3

[17] Merkisz J, Idzior M, Lijewski P, Fuc P, Karpiuk W. The analysis of the quality of fuel spraying in relation to selected rapeseed oil fuels for the common rail system. Proceedings of the Ninth Asia-Pacific International Symposium on Combustion and Energy Utilization. 2008.

[18] Mohd Tamam MQ, Omi MRT, Yahya WJ, Ithnin AM, Abdul Rahman H, Rahman MM et al. Engine performance and emissions evaluation of surfactant-free B30 biodiesel–diesel/water emulsion as alternative fuel. Sci Rep. 2023;13(1):10599. https://doi.org/10.1038/s41598-023-37662-4

[19] Nie G, Li Y, Sheng P, Zuo F, Wu H, Liu L et al. Microstructure refinement-homogenization and flexural strength improvement of Al_2O_3 ceramics fabricated by DLP-stereolithography integrated with chemical precipitation coating process. J Adv Ceram. 2021;10:790-808. https://doi.org/10.21203/rs.3.rs-86507/v1

[20] Niezgoda T, Małachowski J, Szymczyk W. Numerical modelling of the microstructure of ceramics. WNT. Warsaw 2005.
[21] PN-EN 590+A1:2017-06, Automotive fuels – Diesel fuels – Requirements and test methods.
[22] Training materials. Automotive Training Centre, "Autoelectronics Kędzia".
[23] Vengatesan S, Yadav P, Varuvel EG. Effect of alloying elements and ceramic coating on the surface temperature of an aluminum piston in a diesel engine. J Nanomater. 2022; 9916742. https://doi.org/10.1155/2022/9916742
[24] Your Source for Materials Information. MatWeb. www.matweb.com (accessed on 15.09.2023).
[25] Zhang J, Xiao G, Yi M, Chen Z, Zhang J, Chen H et al. Mechanical properties of ZrB2/SiC/WC ceramic tool materials from room temperature to 1100°C and cutting performance. Int J Refract Hard Met. 2021;101:1-7. https://doi.org/10.1016/j.ijrmhm.2021.105697

Prof. Marek Idzior, DSc., DEng. – Faculty of Civil and Transport Engineering, Poznan University of Technology, Poland.
e-mail: *marek.idzior@put.poznan.pl*

Wojciech Karpiuk, DSc., DEng. – Faculty of Civil and Transport Engineering, Poznan University of Technology, Poland.
e-mail: *wojciech.karpiuk@put.poznan.pl*

Rafał Smolec, MEng. – Faculty of Civil and Transport Engineering, Poznan University of Technology, Poland.
e-mail: *rafal.smolec@put.poznan.pl*